Luminescent Photoproducts in UV-Irradiated Ice

VAUGHAN S. LANGFORD,
ALLAN J. MCKINLEY, AND
TERENCE I. QUICKENDEN*

Department of Chemistry, The University of Western Australia, Nedlands, WA 6907, Australia

Received November 12, 1999

ABSTRACT

This Account describes the near-UV and visible luminescences emitted from crystalline, polycrystalline, and amorphous ices as a result of excitation by UV light. Vibrationally resolved, short-lived luminescence around 340 nm arises from excited O_2 formed by the reaction of two O atoms. Long-lived luminescence around 420 nm is tentatively assigned to a spin-forbidden $^4\Sigma^- \rightarrow X\,^2\Pi$ transition of OH. This Account gives a history of the research into this little-known phenomenon, places it in the context of other spectroscopic studies of gaseous and solid water, and proposes future directions for the work.

I. Introduction

The photochemical and photophysical properties of water ice are of such importance and complexity that research interest in this area is increasing. The complexity of the photochemistry and photophysics of ice arises for two reasons. First, the aggregation of isolated water molecules into a solid matrix perturbs their spectroscopic characteristics significantly. Second, significant quantities of photoproducts produced by initial irradiation are trapped in the ice matrix and strongly alter the spectroscopic characteristics of the host, leading to additional absorption features and an even more diverse set of photoproducts. Consequently, the photolysis of ice into hydroxylic species is more probable than would at first be expected from a substance that is often (mistakenly) perceived as being completely transparent from 200 to 700 nm. Photoproducts identified in UV-irradiated ice include O_2,[1] atomic H,[2] OH,[2,3] and H_2O_2.[2]

Interest[4] in the spectral properties of water ice has received a substantial impetus in recent years from its identification on outer solar system bodies (such as Jupiter's Galilean satellites, Europa, Ganymede, and Callisto) and in comets, which are largely comprised of "dirty" ice. The occurrence of ice in extraterrestrial environments is of particular importance because it could allow life to be supported at these remote locations on a permanent basis. Optical techniques for remote identification of ice currently use reflectance spectroscopy, but luminescence spectroscopy is also a possibility.[4]

This Account brings together the published work on the luminescence of UV-excited H_2O and D_2O ices and examines the implications that such work has for the identification and monitoring of photoproducts in an ice matrix. The Account does not cover the luminescences produced in ice excited by electrons and other high-energy radiations. It is believed[5] that the emissions caused by such high-energy radiation result from different mechanisms than those produced by light of wavelength greater than 200 nm, which are the subject of the present Account.

Methods for the Detection of Photogenerated Species in Ice. Definitive assignment of features in the absorption, luminescence, or electron paramagnetic resonance (EPR) spectra of ice is often difficult for several reasons. First, the ice lattice often significantly perturbs photoproducts, such that their absorption and emission lines shift and broaden and their electronic *g* values change. Second, broadening in optical absorption and/or luminescence spectra often obscures fine structure.

Definitive identification of photoproducts may be assisted by the use of several techniques. This strategy was employed to assign the broad absorption band at 280 nm in electron-excited ice (Figure 1a) to the hydroxyl (OH) radical,[6] because the absorption intensity decayed with temperature according to the known[6,7] behavior of EPR-monitored OH. Unfortunately, similar correlations have not yet been made for UV-excited ice.

Ghormley and Hochanadel[2] flash-photolyzed ice at 263 K using a pulsed xenon lamp. Their transient absorption spectra (shown in Figure 1b) revealed $H^\bullet$ and $OH^\bullet$ photoproducts, the former only on the microsecond time scale. HO_2 was not observed. Soon after, Kuwata et al.[8] used EPR to detect photoproducts formed after photolysis of ice by 121.6-nm UV light at 77 K. Their assignment[8] of the EPR to HO_3 is perplexing, since the EPR of high-energy-irradiated ice has not revealed such species.[9,10] Moreover, their EPR spectra of irradiated water vapor,[8] where the formation of HO_3 would be unlikely, look remarkably similar to those of ice. Clarification of this work is necessary. Nevertheless, these reports act as useful point-

Vaughan Langford obtained his Ph.D. in 1997 from the University of Canterbury in Christchurch, New Zealand, under the supervision of Bryce Williamson. His first postdoctoral position was with Andreas Hauser at the University of Geneva, Switzerland. He is currently a University of Western Australia postdoctoral research fellow. His main research interest lies in the optical spectroscopy of matrix-isolated free radicals.

Allan McKinley has research interests in the areas of electron paramagnetic resonance spectroscopy and the degradation and detection of organic contaminants in groundwater. He received his Doctorate in 1986 from the University of Canterbury under the supervision of Dr. R. F. C. Claridge and Professor P. W. Harland. He spent five years in postdoctoral positions with Professor J. Michl at the University of Texas at Austin and Professor R. Metzger at the University of Alabama at Tuscaloosa. He was then a Camille and Henry Dreyfus Fellow with Professor L. Knight, Jr., at Furman University, Greenville, SC, for two years. In 1993 he was appointed at The University of Western Australia and is now a Senior Lecturer in Chemistry.

Terry Quickenden graduated with a Doctorate from the University of Canterbury in New Zealand in 1967 and has published extensively on the luminescence properties of gaseous, liquid, and solid water over the last 30 years. Another area of interest has been that of the ultraweak luminescences of biological systems. In addition, he has contributed significantly to the literature of electrochemistry—particularly in the areas of photoelectrochemistry and solar energy conversion.

* To whom correspondence should be addressed. Fax: +61-8-93801005. E-mail: tiq@chem.uwa.edu.au.

10.1021/ar990145e CCC: $19.00
Published on Web 06/27/2000

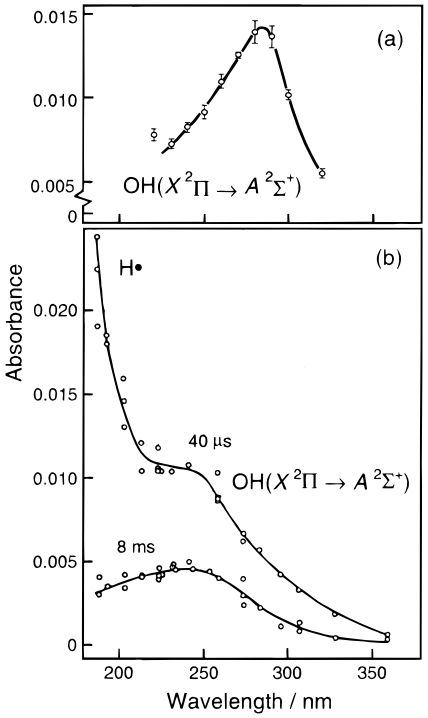

FIGURE 1. (a) UV absorption spectrum of electron-irradiated ice at 175 K. Adapted from ref 6 with permission from Dr. I. A. Taub and the American Institute of Physics. (b) Transient absorption spectra of flash-photolyzed ice at 263 K, obtained 40 μs and 8 ms after the flash. Reprinted with permission from ref 2. Copyright 1971 the American Chemical Society.

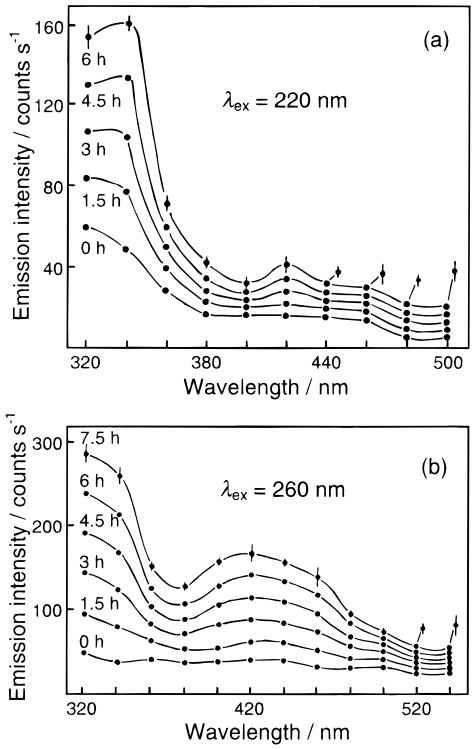

FIGURE 2. Luminescence spectra of UV-irradiated crystalline H_2O ice at 88 K: (a) 220-nm and (b) 260-nm excitation. Accumulation of luminescence intensity is shown as a function of the irradiation time in hours. Reprinted with permission from ref 16. Copyright 1985 Elsevier Science.

ers to the assignment of luminescent photoproducts, although care must be taken in relating these data to the luminophores. For example, species detected by EPR or absorption may not luminesce, or, alternatively, the luminophore may be EPR-inactive or may be below the detection limit of EPR and/or optical absorption spectroscopy. Hence, it is important to relate the UV-excited luminescence of ice to relevant data from a range of sources, including EPR spectroscopy and gas-phase and matrix-isolation optical spectroscopy. Such comparisons form part of this Account.

Our Account is arranged as follows. Section II gives an overview of the ice luminescence literature, dealing sequentially with the distinct luminescence features. New thoughts on the interpretation of the experimental data are offered in section III. In section IV, we summarize the current state of knowledge and suggest future directions for the work on the luminescence of UV-excited ice.

II. History of Studies of Luminescence from UV-Irradiated Ices

Prior to 1970, reports[11−14] of luminescence from UV-excited ice arose from qualitative, visual observations, and neither spectroscopic nor kinetic measurements were made. The water purity was not specified in these early works, and thus it cannot be ascertained whether the luminescence originated from the ice or organic impurities therein.

In 1970, Vierke and Stauff[15] obtained the first quantitative luminescence spectra of ice in experiments designed to detect long-lived (>5 ms) luminescence after 290-nm flash irradiation at 77 K. The luminescence bandwidth was broad and extended from 390 to 600 nm. Superimposed on it were two weak, high-energy peaks and two more intense, low-energy peaks. Vierke and Stauff used highly purified water in their experiments. Hence, their proposal that the observed luminescence was due not to ice, but to the presence of two unknown organic impurities, either airborne or residing on the walls of the sample cuvette, is rather surprising.

Since the work of Vierke and Stauff,[15] UV-excited ice luminescence has been investigated primarily by the Quickenden research group at the University of Western Australia.[1,3,16−19] Results from our first publication[16] are shown in Figure 2. Broad excitation bands at about 220 and 260 nm in crystalline ice gave rise to broad emission bands at about 340 and 420 nm, respectively.[16] These features have appeared consistently in later works, and we retain these wavelength values as subsection titles and band labels, even when their fine-structure components have been resolved or when the peak wavelength shifts slightly with different ice morphology.

Luminescent photoproducts are produced by photolysis of H_2O in the ice lattice and by subsequent photolysis or reactions of these photoproducts. Photolysis occurs at wavelengths greater than 200 nm, despite the fact that the peak absorption of the dissociative $^1A_1$ state of H_2O occurs below 150 nm,[20] because of a weak, broad absorption

tail.[21,22] A similar tail is observed for H_2O in rare-gas matrixes.[23] Thermodynamically,[1] dissociation of H_2O in ice can occur for wavelengths as long as ~270 nm, due to stable trapping of the OH photoproduct in the ice lattice. Hence, ice absorption increases with irradiation time since more strongly absorbing photoproducts, such as OH, accumulate in the ice lattice.

Quickenden and co-workers have given a detailed description of their triple distillation procedure for purifying water.[21] The water has properties characteristic of ultrapure water: a high surface tension,[21] a low level of particulates,[21] and very low UV[21,24] and visible[24] absorptivities (<1 ppb of UV-absorbing impurities). Great care was taken to avoid water contamination when preparing crystalline ice and depositing amorphous and polycrystalline ice under high-vacuum conditions.

Ice Morphology. Three ice morphologies are encountered here: crystalline hexagonal ice I_h, polycrystalline ice I_h, and amorphous (or vitreous) ice.[25] The latter is prepared only by very slow deposition of water vapor onto a surface held at <130 K and is thermally unstable. At higher deposition rates and/or warmer temperatures, polycrystalline ice is formed. Crystalline ice I_h is formed at atmospheric pressure at temperatures from 0 to 273 K. Luminescences from the different ice morphologies will be treated together, since the small variations do not require different interpretations. The primary changes[3] are an increase in luminescence quantum efficiency from crystalline to polycrystalline to amorphous ice and a change in the relative intensities of the 340- and 420-nm emissions.

Small- to medium-sized water clusters of ice (or nanocrystals) show completely different luminescence behavior[26] compared to the bulk forms of ice. Irradiation of water clusters containing up to ~1500 molecules with UV photons from a synchrotron source[26] yielded fluorescence excitation spectra similar to those of the free water molecule, rather than bulk ice.[1,16] The proposed mechanism[26] is given in eq 1. n is the original number of water

$$(H_2O)_n + h\nu \rightarrow (H_2O)_n^* \rightarrow (H_2O)_{n-1} + H_2O^* \rightarrow (H_2O)_{n-1} + OH(A\ ^2\Sigma^+)^* + H \quad (1)$$

molecules in the cluster. The excited OH then emits its characteristic luminescence.

The 340-nm Luminescence of Ice. The 340-nm luminescence of UV-excited ice is excited predominantly at 220 nm (Figure 2).[16] Early work on crystalline H_2O ice by Litjens and Quickenden[17] suggested that the luminescence arose from the $A\ ^2\Sigma^+ \rightarrow X\ ^2\Pi$ transition of OH, red-shifted from the gas phase[27] because of the modified Franck–Condon factors in ice that concomitantly blue-shift the excitation maximum.[6] Both the luminophore's accumulation with increased irradiation time[16] and its thermal behavior[17] were similar to those of EPR-detected OH in high-energy-irradiated ices.[7,9] The luminescence lifetime was shorter than the 12-μs lower limit of the instrumentation,[18] which was consistent with an assignment to OH, since OH has a gas-phase lifetime of ~700 ns.[28] The

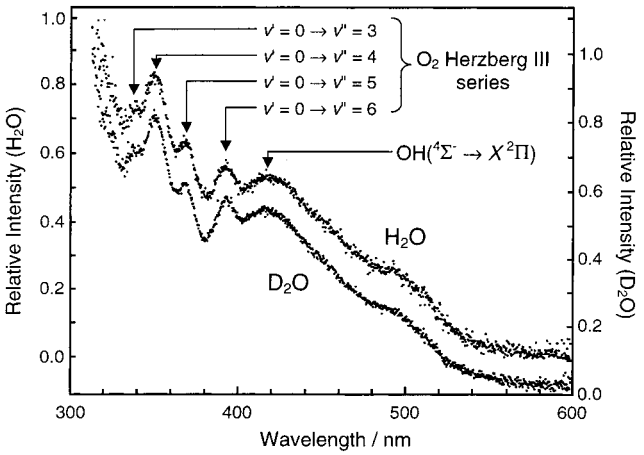

FIGURE 3. Better resolved luminescence spectra of crystalline H_2O and D_2O ice at 78 K, excited by 260-nm light. Features at wavelengths less than ~400 nm are attributed to the Herzberg I or III systems of O_2. Transitions from the upper to lower vibrational states for the Herzberg III system are indicated, as is the tentative assignment of the long-lived 420-nm luminescence to the OH $^4\Sigma^- \rightarrow X\ ^2\Pi$ transition. Reprinted with permission from ref 1. Copyright 1993 the American Chemical Society.

observed linear dependence of luminescence intensity on sample thickness in amorphous and polycrystalline ice indicated a homogeneous distribution of luminophores through the sample.[18]

Figure 3 shows the later work of Matich et al.,[1] which resolved structure not previously observed[16,17] in the UV-excited luminescence of crystalline ice. The broad 340-nm band[16,17] is comprised of four evenly spaced bands that are insensitive to deuterium substitution (Figure 3),[1] and hence the earlier ad hoc assignment[17,29] to OH $A\ ^2\Sigma^+ \rightarrow X\ ^2\Pi$ is invalidated. The structured luminescence was attributed to either the Herzberg I $A\ ^3\Sigma_u^+ \rightarrow X\ ^3\Sigma_g^-$ or Herzberg III $C\ ^3\Delta_u \rightarrow X\ ^3\Sigma_g^-$ systems of O_2 because of the favorable vibrational spacings and their insensitivity to deuterium substitution. The $C\ ^3\Delta_u \rightarrow X\ ^3\Sigma$ transition is dominant in the near-UV luminescence spectra of matrix-isolated O_2[30] and may be the more likely candidate. The $^{16}O_2$ luminescence lifetime in N_2 matrixes decreases from ~250 μs at 4 K to ~25 μs at 14 K.[30] Thus, at 77 K, the lifetime is likely to be less than 12 μs, the upper limit obtained for the ice luminescence lifetime.[18] In ice, the O_2 luminescence is a chemiluminescence of O_2, the intensity growing as O_2 forms. It arises neither from excitation of O_2 trapped in the ice lattice during deposition, nor from re-excitation of the O_2 photoproduct.[1] Two mechanisms for formation of O_2* involve either an O atom and H_2O_2 or two O atoms.[1] The latter is favored due to higher exothermicity. A generalized scheme is shown in eq 2.[1] In this scheme, OH_T and O_m are, respectively,

$$H_2O + h\nu \rightarrow H + OH_T \rightarrow H + O_m \xrightarrow{X_T} O_2^* \rightarrow O_2 + h\nu' \quad (2)$$

trapped OH radicals and mobile O atoms. X_T is trapped H_2O_2 or O. Predissociation in the $A\ ^2\Sigma^+$ state of OH can account for efficient formation of O atoms in UV-irradiated ice (section III).

Table 1. Characteristics of Long-Lived Luminescences from UV-Excited Pure and Doped Ices and Metal Hydroxide Crystals

			luminescence lifetime/s		
sample	temperature/K	band maximum/nm	component a	component b	ref
crystalline ice	88	420	1.7 ± 0.2		29
	77	430	5		32
	77	417	1.9		1
amorphous ice	78	410, 475	1.6 ± 0.1	4.2 ± 0.3	3
polycrystalline ice	78	420	0.8 ± 0.1	2.5 ± 0.4	19
0.1 M $NaOH/H_2O$	77	400	0.9	2.9	33
	?	400	1.35		35
8 M $NaOH/H_2O$	77	400	1.1		34
0.1 M NaOH/MeOH	?	400			35
0.1 M $NaOD/D_2O$	?	390	1.55		35
8 M KOH/H_2O	77	400	0.9		34
$KBr:OH^-$	77	400	0.63	0.2	33
$Ba(OH)_2 \cdot 2H_2O$	77	400	2.0		34
10 M H_2SO_4/H_2O	?	410	1.2		35
1 M H_3PO_4/H_2O	?	410	1.2		35
10 M HF/H_2O	?	410	1.2		35

The above evidence[1,16−18,29] strongly supports assignment of the 340-nm luminescence to the Herzberg I or III systems of O_2.[1] The temperature dependence[17,29] of this band follows closely that of the OH radical in ice, because OH is the source of O atoms. However, it is unclear whether other broad luminescence bands having lifetimes and thermal behavior similar to those of O_2 might underlie the O_2 emission. The OH $A\ ^2\Sigma^+ \rightarrow X\ ^2\Pi$ luminescence is a possible candidate, although in this case isotopic effects would have been expected and should have been detected, unless the OH emission was only a small component of the total luminescence.

The 420-nm Luminescence of Ice. Quickenden and co-workers[16] first observed the 420-nm luminescence of UV-irradiated crystalline H_2O ice at 88 K and found that it was excited primarily at 260 nm (Figure 2). The band was blue-shifted by 1.4 nm in D_2O ice.[1] In amorphous ice, the band was resolved into two components centered at 410 and 475 nm.[3]

The luminescent photoproduct (or its precursor) that leads to the 420-nm emission was found to accumulate[29] in the ice lattice at liquid N_2 temperature, where it survived for at least several hours and was re-excited by further irradiation.

The 420-nm luminescence has a long lifetime of the order of 1 s but varies somewhat with ice morphology (Table 1). The lifetime is insensitive to deuterium substitution in crystalline ice.[31] Early work[1,29] fits the data to second-order kinetics, but the identical rise and fall of luminescence intensity[3] is better represented by biexponential kinetics.[3] The two components of the luminescence derived from the biexponential fit are tentatively attributed to the same luminophore occupying substitutional and interstitial sites in the ice lattice,[3] with the former, shorter-lived component persisting at higher temperatures.[19] Arrhenius treatment of the temperature dependence of the luminescence decay in polycrystalline ice[19] showed that the decay had negligible activation energy, which is consistent with the rate-determining step being an electronic transition, rather than a chemical step.

Khusnatdinov and Petrenko[32] have detected similar 420-nm luminescence from crystalline ice excited between 180 and 300 nm, but they have not reported the 340-nm emission. Their decay data were fitted with a single-exponential expression, yielding a lifetime of 5 s, which is somewhat longer than our data for crystalline ice (Table 1).[1,29]

The 420-nm luminescence was originally tentatively assigned to the OH $A\ ^2\Sigma^+$ ($v = 0$) $\rightarrow X\ ^2\Pi$ ($v = 2$) transition.[17] Later work showed that this assignment was unsatisfactory because the band energy was almost the same for H and D isotopes,[1] contrary to expectations.[27] Furthermore, there was no isotopic effect on luminescence lifetime.[31] Khusnatdinov and Petrenko[32] assigned the luminescence to decay from a low-lying triplet state of H_2O, but this assignment is very unlikely according to work by Quickenden and Irvin.[21] A more recent and much more satisfactory assignment[3] has been to the spin-forbidden $^4\Sigma^- \rightarrow X\ ^2\Pi$ transition of OH, which is likely to be long-lived. Maria and McGlynn[33] first made the $^4\Sigma^- \rightarrow X\ ^2\Pi$ assignment to the long-lived 400-nm luminescences from hydroxide-doped alkali halides and frozen aqueous metal hydroxide solutions excited by UV light. Their data are summarized in Table 1. Subsequent literature, while disagreeing with this assignment,[34,35] has not provided a convincing alternative.[29,31] Quickenden and co-workers[3,19] have adopted the $^4\Sigma^- \rightarrow X\ ^2\Pi$ assignment for the 420-nm luminescence of UV-excited ice because the negligible activation energy and long lifetime suggest that an electronic transition is rate-determining.

Although the $^4\Sigma^-$ state of OH is dissociative in the gas phase,[36,37] Quickenden et al.[3,19] propose that it becomes bound in the ice lattice. This proposal does not appear unreasonable because the ice lattice strongly perturbs OH (section III). A high-level calculation of the $^4\Sigma^-$ state's potential energy (PE) curve in ice and/or direct detection of the $^4\Sigma^-$ state by EPR are necessary before a definitive statement can be made regarding the assignment's validity.

III. New Perspectives

In this section, the ice luminescence results of section II are interpreted with the help of the well-known gas-phase

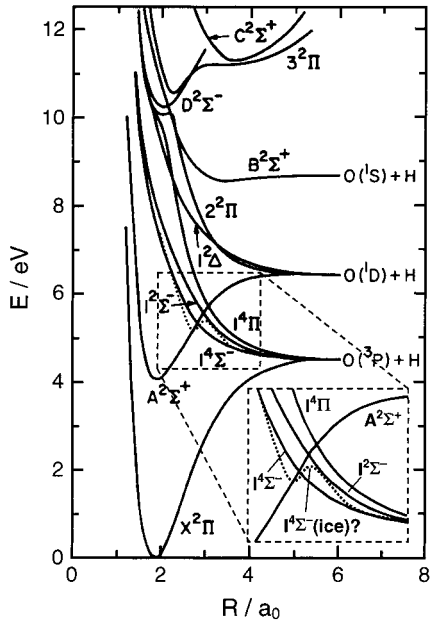

FIGURE 4. Potential energy curves for OH taken from ref 40, except for the dotted curve, which is a hypothetical curve for a bound $^4\Sigma^-$ state in ice. The region of the important crossings is enlarged for clarity.

predissociations of OH $A\ ^2\Sigma^+$. This is then followed by an attempt to draw together the optical and EPR experimental results for OH in a variety of environments as we seek to understand the absence of the normally ubiquitous $A\ ^2\Sigma^+ \rightarrow X\ ^2\Pi$ luminescence when OH is embedded in ice.

Predissociation of OH $A\ ^2\Sigma^+$. In the gas phase, repulsive $^4\Sigma^-$, $^2\Sigma^-$, and $^4\Pi$ states of OH efficiently predissociate the $A\ ^2\Sigma^+$ state for vibrational levels $v > 1$ (Figure 4).[37−40] The $^4\Sigma^-$ state is responsible for the lowest-energy predissociation[40] of the $A\ ^2\Sigma^+$ state at ~38 000 cm^{-1} (262 nm),[28] with a predissociation probability that is a few times greater than the radiative decay probability.[39] The higher-lying $^2\Sigma^-$ and $^4\Pi$ states are ~900 cm^{-1} apart[37] and predissociate the $A\ ^2\Sigma^+$ state at $v \approx 5$, or ~46 000 cm^{-1} (217 nm) above the ground state.[37,38,40] The predissociation induced by the $^4\Pi$ state is very strong,[38] reducing the lifetimes of rovibrational levels to ~10^{-11}−10^{-12} s.[38,41] Because of the small separation between the $^2\Sigma^-$ and $^4\Pi$ states and the broad OH absorption bands in ice, we do not consider the $^2\Sigma^-$ predissociation here.

The situation for OH in ice may well be somewhat modified. If the $^4\Sigma^-$ state is made associative by the ice matrix, as proposed by Quickenden et al.,[3,19] a reasonably efficient pathway for the preparation of OH($^4\Sigma^-$) should be accessible at ~260 nm, although the crossing energy may be shifted from its gas-phase value. Dissociation of OH is prevented if the crossing point of the $A\ ^2\Sigma^+$ and $^4\Sigma^-$ states corresponds to a bound portion of the $^4\Sigma^-$ PE curve. With these constraints in mind, a possible form for a bound $^4\Sigma^-$ state is shown as the dotted curve in Figure 4. Figure 5 shows a schematic Jablonski diagram summarizing the proposed pathway to the luminescence, which terminates at $v \approx 4$ of the $X\ ^2\Pi$ state.[33] A calculation of the PE curves of OH in ice would, indeed, be most helpful but is not available at present.

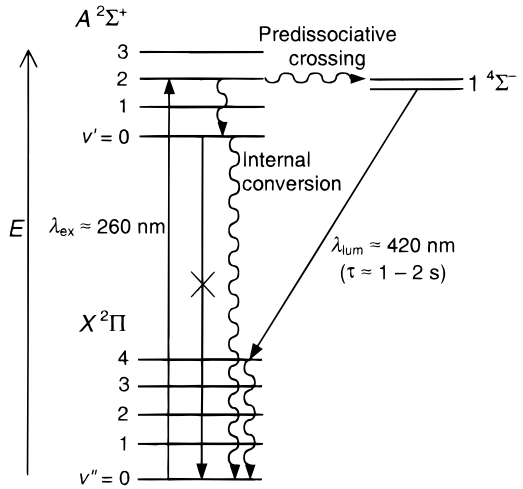

FIGURE 5. Schematic Jablonski diagram showing the proposed processes leading to OH $^4\Sigma^- \rightarrow X\ ^2\Pi$ luminescence in ice and the absence of $A\ ^2\Sigma^+ \rightarrow X\ ^2\Pi$ luminescence.

The strong predissociation of the $A\ ^2\Sigma^+$ state by the $^4\Pi$ state ensures that a large number of O atoms are formed when OH is excited to $A\ ^2\Sigma^+$ ($v \approx 5$). The yield will be moderated somewhat by small Franck−Condon overlap for OH $X\ ^2\Pi$ ($v = 0$) → $A\ ^2\Sigma^+$ ($v = 5$) absorption, but the shift of the absorption maximum from 306 nm[27] in the gas phase to 280 nm[6] in ice suggests that overlap is greater in ice. The $^4\Pi$ predissociation occurs at an energy very similar to that of the peak of the ice excitation spectrum when it is detected in the O_2 luminescence (340 nm; section II). Thus, the strong predissociation of OH $A\ ^2\Sigma^+$ by $^4\Pi$ is very probably responsible for more efficient production of O atoms at ~220 nm than at longer wavelengths. A higher concentration of O atoms leads to more O_2* and hence to more intense 340-nm luminescence.

Predissociation of OH $A\ ^2\Sigma^+$ by $^4\Sigma^-$ and $^4\Pi$ states supports the observed[16] relationship of 220- and 260-nm excitation to 340- and 420-nm emissions, respectively. At shorter wavelengths there is a higher yield of O atoms that gives rise to the O_2 luminescence around 340 nm.[1] At longer excitation wavelengths, more OH crosses to the bound portion of the $^4\Sigma^-$ potential curve (Figure 4), giving greater intensity to the 420-nm band assigned to the OH $^4\Sigma^- \rightarrow X\ ^2\Pi$ transition.[3,19]

The Intriguing Absence of OH $A\ ^2\Sigma^+ \rightarrow X\ ^2\Pi$ luminescence. If the recent assignments of the 340- and 420-nm luminescence bands to the respective Herzberg and $^4\Sigma^-$ transitions are indeed correct, this removes the well-known and often dominant $A\ ^2\Sigma^+ \rightarrow X\ ^2\Pi$ emission of OH from consideration in UV-excited ice (Figure 5). Furthermore, it is now known[5] that above 77 K the emissions from electron-excited ice are dominated by the $C\ ^1B_1 \rightarrow A\ ^1B_1$ excimer transition of H_2O and not the $A\ ^2\Sigma^+ \rightarrow X\ ^2\Pi$ transition of OH. We note that the $^4\Sigma^-$ predissociation of the $A\ ^2\Sigma^+$ state cannot totally quench this luminescence because, at its strongest, the predissociation probability is only a few times greater than the luminescence probability.[39] EPR and luminescence data reveal that OH trapped in ice is very different from OH in the gas phase, where the $A\ ^2\Sigma^+ \rightarrow X\ ^2\Pi$ transition is so dominant.

Table 2. Optical Absorption and Luminescence Data for the OH $A\ ^2\Sigma^+ - X\ ^2\Pi$ Transition in Various Media

		(0,0) luminescence		
medium	(0,0) absorption/ nm	maximum/ nm	lifetime/ ns	quantum efficiency
gas phase	306.4[27]	306.4[27]	693 ± 20[28]	~1
Ne matrix[46]	308.1	309.1	582 ± 10	>0.9
Ar matrix[47]	310.8	340	475 ± 10	>0.9
Kr matrix[47]	*a*	363	450 ± 20	>0.9
Xe matrix[47]	*a*	440	100 ± 4	>0.9
KCl[33]	*b*	300	*c*	*c*
KBr[33]	*b*	311	*c*	*c*
ice	280[6]	*d*	*d*	*d*

[a] Not stated. [b] Below detection limit. [c] Not measured. [d] Absent.

Consider first the EPR data. The EPR of gas-phase OH gives an orbital angular momentum g value (g_l) of unity for the electronic ground state of OH.[42] Detection of OH in ice by EPR after β-,[7,9] γ-,[43,44] or X-irradiation[10] is well documented. The measured g value is very close to that of a free electron, and thus the orbital angular momentum is almost completely quenched[9,43] ($g_l \approx 0$). Quenching occurs because hydrogen bonding of the OH radical to H_2O molecules of the ice lattice lowers the degeneracy of the OH p_x and p_y orbitals.[43,45]

Consider now the $A\ ^2\Sigma^+ \rightarrow X\ ^2\Pi$ luminescence of OH, which might be expected from UV-irradiated ices because H and OH radicals are probably the only primary photoproducts formed at excitation wavelengths greater than 200 nm.[1] The abundance of rovibrational levels in $A\ ^2\Sigma^+$ should mean that once formed, OH would be relatively easily excited into one of these levels and the characteristic luminescence observed. This is *not* the case in ice, as we have seen above.

Table 2 summarizes the optical luminescence data for OH $A\ ^2\Sigma^+ \rightarrow X\ ^2\Pi$ in a variety of environments. The well-known gas-phase $A\ ^2\Sigma^+ \rightarrow X\ ^2\Pi$ emission of OH[27,28] is observed when OH is embedded in rare-gas matrixes.[46,47] The luminescence quantum yield remains high despite OH being increasingly perturbed by weak hydrogen bonding to a rare-gas atom[47] along the series Ne,[46] Ar,[47] Kr,[47] and Xe.[47] OH luminescence is also observed from UV-irradiated alkali halide crystals containing a small amount of alkali hydroxide.[33] The (0,0) and (0,1) transitions are little shifted from their gas-phase values.

The absence of the OH $A\ ^2\Sigma^+ \rightarrow X\ ^2\Pi$ emission in ice is not due to the crystal field imposed by the ice lattice, because then quenching would occur to some extent in alkali halides and rare-gas matrixes. OH in Ar matrixes exhibits partial quenching of orbital angular momentum in some sites,[48] due very likely to weak hydrogen bonding of OH to an Ar atom, which is insufficiently strong to quench luminescence.[47] OH $A\ ^2\Sigma^+ \rightarrow X\ ^2\Pi$ emission is apparently quenched in ice by strong hydrogen bonding of OH to water molecules of the ice lattice. The quenchings of both luminescence and orbital angular momentum are evidently related.

Miyazaki et al.[49,50] have observed OH $A\ ^2\Sigma^+ \rightarrow X\ ^2\Pi$ emission from electron-irradiated ice at temperatures lower than 77 K. However, this emission arises from OH $A\ ^2\Sigma^+$ formed by dissociative recombination of H_2O^+ and e^-, which is significant only below 77 K.[50] The emitting OH radicals are not the stably trapped OH observed by EPR, because they do not show the known persistence to temperatures above 100 K.[6,7]

Finally, since the hydrogen bonding of OH to H_2O in ice has a profound effect on both the orbital angular momentum of OH ($X\ ^2\Pi$) and the $A\ ^2\Sigma^+ \rightarrow X\ ^2\Pi$ luminescence, it may indeed not be surprising that the repulsive $^4\Sigma^-$ state becomes bound.[3,19]

IV. Summary and Outlook

We have reviewed the published studies of UV-excited ice luminescence. The assignment of the 340-nm luminescence band to the Herzberg I or III systems seems entirely reasonable. The resolved structure has spacings corresponding to O_2 vibrations, the spacings are not affected by deuterium substitution for hydrogen, and the lifetime is in the correct range. Measurement of the decay kinetics should reveal the luminescence lifetime and provide a new test of the mechanism for O_2 production. Excitation at ~220 nm leads to efficient predissociation of OH, producing O atoms that react to give chemiluminescent O_2. Hence, the temperature dependence of the O_2 luminescence is similar to that of the OH radical. It remains to be seen whether other luminescence bands underlie the O_2 structure. If they do, their temperature dependence is evidently similar to that of O_2, and they, like O_2, have a lifetime shorter than 12 μs. Measurement of the temperature dependence of the luminescence decay may answer this question.

Assignment of the 420-nm luminescence remains less certain. Many aspects of its behavior could correspond to the spin-forbidden $^4\Sigma^- \rightarrow X\ ^2\Pi$ transition of OH. The $^4\Sigma^-$ state is dissociative in the gas phase but is proposed to become associative in ice. The long luminescence lifetime and zero activation energy for the process provide support for this proposal. However, the temperature dependence of the band differs from that of OH by steadily decreasing with increasing temperature, whereas OH detected by EPR disappears very suddenly between 100 and 130 K. Early work proposed that a stable precursor to OH, for example H_2O_2, could be responsible for such behavior. Soon, we intend to use EPR as a probe for OH and other EPR-active photoproducts. Support for a bound $^4\Sigma^-$ state of OH embedded in ice might also be provided by high-level theoretical calculations.

The absence of OH $A\ ^2\Sigma^+ \rightarrow X\ ^2\Pi$ luminescence in ice is intriguing and warrants further study. Shortly, we will undertake matrix-isolation experiments to probe the OH luminescence behavior when it is embedded in water clusters of varying size. These experiments should provide valuable insight into the nature of the luminescence quenching and possibly show the $^4\Sigma^-$ emission in the hydrogen-bonded environment. Measurement of the UV-excited luminescence of water clusters embedded in solid, inert environments may provide data in closer agreement

with those from bulk ice than were obtained by transient excitation of gas-phase clusters.

A.J.M. and T.I.Q. are grateful for research support from the Australian Research Council and the University of Western Australia. V.S.L. gratefully acknowledges the tenure of a University of Western Australia postdoctoral research fellowship. We thank a reviewer for many helpful comments.

References

(1) Matich, A. J.; Bakker, M. G.; Lennon, D.; Quickenden, T. I.; Freeman, C. G. O_2 luminescence from UV-excited H_2O and D_2O ices. *J. Phys. Chem.* **1993**, *97*, 10539−10553.
(2) Ghormley, J. A.; Hochanadel, C. J. Production of H, OH, and H_2O_2 in the flash photolysis of ice. *J. Phys. Chem.* **1971**, *75*, 40−44.
(3) Quickenden, T. I.; Green, T. A.; Lennon, D. Luminescence from UV-irradiated amorphous H_2O ice. *J. Phys. Chem.* **1996**, *100*, 16801−16807.
(4) Johnson, R. E.; Quickenden, T. I. Photolysis and radiolysis of water ice on outer solar system bodies. *J. Geophys. Res.* **1997**, *102*, 10985−10996.
(5) Vernon, C. F.; Matich, A. J.; Quickenden, T. I.; Sangster, D. F. Isotopic effects on the decay kinetics of the 385-nm luminescence from electron-irradiated ice. *J. Phys. Chem.* **1991**, *95*, 7313−7319.
(6) Taub, I. A.; Eiben, K. Transient solvated electron, hydroxyl and hydroperoxy radicals in pulse-irradiated crystalline ice. *J. Chem. Phys.* **1968**, *49*, 2499−2513.
(7) Kroh, J.; Green, B. C.; Spinks, J. W. T. Electron paramagnetic resonance studies on free radicals produced by Tβ-particles in frozen H_2O and D_2O media at liquid nitrogen temperature. *Can. J. Chem.* **1962**, *40*, 413−425.
(8) Kuwata, K.; Kotake, Y.; Inada, K.; Ono, M. Electron spin resonance study of the far-ultraviolet photolysis of some inorganic and organic compounds. *J. Phys. Chem.* **1972**, *76*, 2061−2069.
(9) Gunter, T. E. Electron paramagnetic resonance studies of the radiolysis of H_2O in the solid state. *J. Chem. Phys.* **1967**, *46*, 3818−3829.
(10) Box, H. C.; Budzinski, E. E.; Lilga, K. T.; Freund, H. G. ENDOR study of *X*-irradiated single crystals of ice. *J. Chem. Phys.* **1970**, *53*, 1059−1065.
(11) Kayser, H. *Handbuch der Spectroscopie*; Hirzel: Liepzig, 1900; pp 636, 686, 832.
(12) Armstrong, H. E. Problems of hydrone, etc. Luminous ice. *Nature* **1924**, *113*, 163.
(13) Wick, F. G. The triboluminescence of sugar and ice. *J. Opt. Soc. Am.* **1940**, *30*, 91−92.
(14) Wick, F. G. Triboluminescence of sugar. *J. Opt. Soc. Am.* **1940**, *30*, 302−306.
(15) Vierke, G.; Stauff, J. Zur lumineszenz des eises. *Ber. Bunsen-Ges. Phys. Chem.* **1970**, *74*, 358−364.
(16) Quickenden, T. I.; Litjens, R. A. J.; Freeman, C. G.; Trotman, S. M. UV excited luminescence from crystalline ice. *Chem. Phys. Lett.* **1985**, *114*, 164−167.
(17) Litjens, R. A. J.; Quickenden, T. I. Studies of UV stimulated luminescence from H_2O ice. *J. Phys., Colloq. C1* **1987**, *48*, 59−65.
(18) Lennon, D.; Quickenden, T. I.; Freeman, C. G. UV-excited luminescences from amorphous and polycrystalline H_2O ices. *Chem. Phys. Lett.* **1993**, *201*, 120−126.
(19) Quickenden, T. I.; Hanlon, A. R.; Freeman, C. G. Activation energy for the emission of 420 nm luminescence from UV-excited polycrystalline H_2O ice. *J. Phys. Chem. A* **1997**, *101*, 4511−4516.
(20) Dressler, K.; Schnepp, O. Absorption spectra of solid methane, ammonia and ice in the vacuum ultraviolet. *J. Chem. Phys.* **1960**, *33*, 270−274.
(21) Quickenden, T. I.; Irvin, J. A. The ultraviolet absorption spectrum of liquid water. *J. Chem. Phys.* **1980**, *72*, 4416−4428.
(22) Bursulaya, B. D.; Jeon, J.; Yang, C.-N.; Kim, H. J. On the photoabsorption spectroscopy of water. *J. Phys. Chem. A* **2000**, *104*, 45−52.
(23) Schriever, R.; Chergui, M.; Kunz, H.; Stepanenko, V.; Schwentner, N. Cage effect for the abstraction of H from H_2O in Ar matrices. *J. Chem. Phys.* **1989**, *91*, 4128−4133.
(24) Litjens, R. A. J.; Quickenden, T. I.; Freeman, C. G. Visible and near-ultraviolet absorption spectrum of liquid water. *Appl. Opt.* **1999**, *38*, 1216−1223.
(25) Hobbs, P. V. *Ice Physics*; Clarendon: Oxford, 1974.
(26) Ahmed, M.; Apps, C. J.; Hughes, C.; Whitehead, J. C. Vacuum ultraviolet excitation of large water clusters. *J. Phys. Chem.* **1994**, *98*, 12530−12534.
(27) Huber, K. P.; Herzberg, G. *Molecular Spectra and Molecular Structure, Volume 4: Constants of Diatomic Molecules*; van Nostrand Reinhold: New York, 1979.
(28) German, K. R. Radiative and predissociative lifetimes of the $v' = 0$, 1 and 2 levels of the $A\ ^2\Sigma^+$ state of OH and OD. *J. Chem. Phys.* **1975**, *63*, 5252−5255.
(29) Litjens, R. A. J. Luminescence from H_2O Ice Excited by Electrons and Ultraviolet Light. Ph.D. Thesis, The University of Western Australia, Perth, 1986.
(30) Goodman, J.; Brus, L. E. Electronic spectroscopy and dynamics of the low-lying $A\ ^3\Sigma_u^+$, $C\ ^3\Delta_u$ and $c\ ^1\Sigma_u^-$ states of O_2 in van der Waals solids. *J. Chem. Phys.* **1977**, *67*, 1482−1490.
(31) Matich, A. J. Luminescence from Ultraviolet and Electron Irradiated Ice. Ph.D. Thesis, The University of Western Australia, Perth, 1992.
(32) Khusnatdinov, N. N.; Petrenko, V. F. Photoluminescence of ice-I_h in a spectral region 180−300 nm. In *Physics and Chemistry of Ice*; Maeno, N., Hondoh, T., Eds.; Hokkaido University Press: Sapporo, 1992; pp 163−169.
(33) Maria, H. J.; McGlynn, S. P. Luminescence of systems containing hydroxyl ion. *J. Chem. Phys.* **1970**, *52*, 3402−3408.
(34) Merkel, P. B.; Hamill, W. H. Evidence for a low-lying triplet state of the hydroxide ion. *J. Chem. Phys.* **1971**, *55*, 2174−2177.
(35) Mathers, T. L.; Nauman, R. V.; McGlynn, S. P. Low-temperature luminescence of aqueous systems. *Chem. Phys. Lett.* **1986**, *126*, 408−412.
(36) Bazet, J. F.; Harel, C.; McCarroll, R.; Riera, A. Electronic energies including exchange and spin−orbit interaction of the interstellar molecules CH^+, CH and OH at large interatomic separations. *Astron. Astrophys.* **1975**, *43*, 223−228.
(37) Yarkony, D. R. A theoretical treatment of the predissociation of the individual rovibronic levels of OH/OD($A\ ^2\Sigma^+$). *J. Chem. Phys.* **1992**, *97*, 1838−1849.
(38) Czarny, J.; Felenbok, P.; Lefebvre-Brion, H. High vibrational level predissociation in the $A\ ^2\Sigma^+$ state of OD. *J. Phys. B* **1971**, *4*, 124−132.
(39) Brzozowski, J.; Erman, P.; Lyrra, M. Precision estimates of the predissociation rates of the OH $A\ ^2\Sigma^+$ state ($v \leq 2$). *Phys. Scr.* **1978**, *17*, 507−511.
(40) Kirby, K. P.; van Dishoeck, E. F. Photodissociation processes in diatomic molecules of astrophysical interest. *Adv. Atom. Mol. Phys.* **1998**, *25*, 437−476 and references therein.
(41) Carlone, C.; Dalby, F. W. Spectrum of the hydroxyl radical. *Can. J. Phys.* **1969**, *47*, 1945−1957.
(42) Radford, H. E. Microwave Zeeman effect of free hydroxyl radicals. *Phys. Rev.* **1961**, *122*, 114−130.
(43) Dibdin, G. H. ESR of γ-irradiated single crystals of ice at 77°K. *Trans. Faraday Soc.* **1967**, *63*, 2098−2111.
(44) Symons, M. C. R. Electron spin resonance studies of OH and O^- radicals in irradiated ice. *J. Chem. Soc., Faraday Trans. 1* **1982**, *78*, 1953−1959.
(45) Riederer, H.; Hütterman, J.; Boon, P.; Symons, M. C. R. Hydroxyl radicals in aqueous glasses: Characterization and reactivity studied by ESR spectroscopy. *J. Magn. Reson.* **1983**, *54*, 54−66.
(46) Brus, L. E.; Bondybey, V. E. Pseudorotational local mode participation in OH and OD($A\ ^2\Sigma^+$) vibrational relaxation in a Ne lattice. *J. Chem. Phys.* **1975**, *63*, 786−793.
(47) Goodman, J.; Brus, L. E. Hydrogen bonding and charge transfer: Interaction of OH radical with rare gas atoms. *J. Chem. Phys.* **1977**, *67*, 4858−4865.
(48) Langford, V. S.; Williamson, B. E. Magnetic circular dichroism of the hydroxyl radical in an argon matrix. *J. Phys. Chem. A* **1997**, *101*, 3119−3124.
(49) Miyazaki, T.; Kamiya, Y.; Fueki, K.; Yasui, M. New band of emission from high-energy-electron-irradiated ice at very low temperature. *J. Phys. Chem.* **1992**, *96*, 9558−9561.
(50) Miyazaki, T.; Nagasaka, S.; Kamiya, Y.; Tanimura, K. Formation of excited OH radicals in high-energy-electron-irradiated ice at very low temperature. *J. Phys. Chem.* **1993**, *97*, 10715−10719.

AR990145E